Approximate Quantum Mechanical Cross Sections and Rate Constants for the H + O_3 Atmospheric Reaction Using Novel Elastic Optimum Angle Adiabatic Approaches

H. Szichman[†] and A. J. C. Varandas*

Departamento de Química, Universidade de Coimbra, 3049 Coimbra Codex, Portugal

Received: November 13, 1998; In Final Form: January 27, 1999

Three-dimensional quantum dynamics computations of cross sections and rate constants for the atmospheric reaction H + O_3 → O_2 + OH are presented. Using a novel elastic optimum angle adiabatic approach published in a previous paper (Varandas, A. J. C.; Szichman, H. *Chem. Phys. Lett.* **1998**, *295*, 113), the calculated cross sections cover the range of translational energies $0.035 \leq E_{tr}/eV \leq 0.300$. Applications of the new approach using both single-path and multiple-path schemes are reported. The results are compared with available classical trajectory and infinite-order-sudden-approximation results. It may be concluded that the calculations obtained from the single-path model give an improved agreement with respect to the sudden ones when compared with the classical trajectory results. In turn, the quantum elastic optimum angle adiabatic multiple-path results show excellent agreement with the same classical results.

1. Introduction

The reduced dimensionality treatment is, and will remain to be in the forseeable future, the most feasible method to carry out quantum mechanical (QM) studies in polyatomic systems. So far, accurate QM computations can be done on systems including up to three atoms, such as the prototypical reactions H + H_2 (and its isotopomers),[1,2] F + H_2,[3] as well as O + H_2,[4] Cl + H_2,[5] and other atom−diatom reactions.[6] In some favorable cases of tetra-atomic systems such as $H_2(D_2)OH$[7−10] or $H_2(D_2)$-CN,[11] it has also been possible to perform full six-dimensional (6D) QM treatments. These tetra-atomic systems are characterized by having the OH or CN diatomic fragments in a state of *spectators* during the reactive process, which reduces in practice the computational complexity to that of a 5D problem. In turn, for $H_2(D_2)OH$, the adjacency of the O atom to the center of mass gives to this system a nearly coplanar symmetry, for which a 4D QM treatment can yield quite reasonable results.[12] It is quite clear though that if a time-dependent 6D formalism such as that used in ref 9 is used to treat the title reaction or other important atmospheric reactions such as

$$O + HO_2 \rightarrow OH + O_2,\ \Delta H_{class} = -51.94\ \text{kcal mol}^{-1} \qquad (1)$$

then the required computing resources would certainly fall far ahead from those necessary to treat the above-mentioned tetra-atomic systems; ΔH_{class} is the classical enthalpy of reaction. Indeed, even if there is (or soon becomes available) the high technology required to find the QM full solution of reaction (eq 1), it is doubtful whether it will be readily available to treat a wealth of interesting and useful chemical reactions, such as the title one, not to mention the more complex and perhaps exciting (yet almost unexplored) systems involving five or more atoms.

The continuing development of novel computational approaches to carry out QM reduced dimensionality studies of polyatomic systems remains therefore a must. In this sense, the authors have already published a novel method based on adiabatic principles,[13] which intends to cover the computation of reaction probabilities in low translational energy regimes, where the known infinite-order-sudden-approximation (IOSA)[14] method has been shown to give systematically lower values than those predicted by other theories such as QCT.[13,15] The development of this adiabatic path approach[13] has led to the introduction of two alternative schemes of reaction probability averaging, i.e., the *elastic optimum angle adiabatic single (multiple) path* techniques, EOAAS(M)P, the first of which (EOAASP) has already been applied[13] to reaction 1; for brevity, their acronyms will be referred to heretofore in an obvious correspondence as SP and MP. In the present paper we explore the S(M)P approaches in the study of another important atmospheric reaction, namely

$$H + O_3 \rightarrow HO + O_2,\ \Delta H_{class} = -81.0\ \text{kcal mol}^{-1} \qquad (2)$$

In so doing we are aware of the 3-fold difficulties inherent to reaction 2 which were absent in the treatment of reaction 1, namely (1) Two optimum directions for the H atom to attack the ozone molecule[15−18] rather than just one for O to attack the HO_2 radical in the case of reaction 1.[13] (2) Two open reaction channels[15,16,18] rather than only one as in reaction 1. (3) A classical enthalpy of reaction almost twice as large as that of reaction 1. To cope with the above-mentioned difficulties, we have therefore developed new principles within the S(M)P approaches which allow us to achieve more reliable results.

2. Theory

Our method is based on the calculation of all nonreactive probabilities, $\mathbf{P}(\lambda \leftarrow \lambda_0)$ the sum of which is then subtracted from unity to obtain the total reactive probability. Thus,

$$P^J_{\text{react}} = 1 - \sum_{\lambda} |S^J(\lambda - \lambda_0)|^2 \qquad (3)$$

where $S^J(\lambda \leftarrow \lambda_0)$ is an element of the nonreactive scattering

* Author to whom correspondence should be addressed.
[†] On leave from the Department of Physics and Applied Mathematics, Soreq NRC, Yavne 81800, Israel.

10.1021/jp984434g CCC: $18.00
Published on Web 03/13/1999

$\mathbf{S}^{\mathbf{J}}$-matrix, and λ (and λ_0) stand for a set of quantum numbers which label a state of the four-atom system. It is understood that since each reactive process is characterized by a constant total angular momentum quantum number J, one may drop this from the notation henceforth. If $\tilde{\mathbf{S}}$ is the ordinary transition (reactive) matrix, the **S**-matrix may be written as[19]

$$\mathbf{S} = \mathbf{I} - \tilde{\mathbf{S}} \tag{4}$$

where **I** is the unity matrix.

Prior to the calculation of the S-matrix terms, the following Schrödinger equations (SEs) must be solved, namely

$$(E - H)\Psi_{\lambda_0} = 0 \tag{5}$$

and

$$(E - H_0)\psi_\lambda = 0 \tag{6}$$

where Ψ_{λ_0} is the complete wave function associated with the asymptotic state λ_0, and ψ_λ represents the λth quantum mechanical solution of the unperturbed (elastic) SE, eq 6; H and H_0 are, respectively, the full and unperturbed Hamiltonians describing the atom−triatom system.

Assuming the unpertubed solution ψ_{λ_0} to be known, by using the perturbative method, the full solution Ψ_{λ_0} may then be written as

$$\Psi_{\lambda_0} = \psi_{\lambda_0} + \chi_{\lambda_0} \tag{7}$$

where it can be easily shown that χ_{λ_0} can be obtained by solving the following inhomogenuous SE in the close-interaction region

$$(E - H_I)\chi_{\lambda_0} = V\psi_{\lambda_0} \tag{8}$$

with V being the interaction (perturbation) potential defined by

$$V = H - H_0 \tag{9}$$

Thus, as mentioned above, H is the full Hamiltonian and H_I is ad-hoc obtained by adding negative imaginary potentials (NIPs) to H; these are defined along the boundaries of the arrangement channel (AC) in which ψ_{λ_0} is calculated. As usual, the function of these NIPs is to decouple one arrangement channel from all others, and provide bound-state-like boundary conditions.[20]

As already done in previous reports on the same title reaction,[15,16] a Jacobi coordinate system has been used in the present work to describe both ACs of the four-atom system (see Figure 2 of ref 15). Thus, the atom−triatom (reagent) channel is described by three radial distances and three Jacobi angles. The former include the vibrational coordinate for the unbroken bond r, the corresponding "translational" coordinate of the triatom ρ connecting the third atom with the center of mass of the unbroken bond, and the translational coordinate R which connects the fourth atom to the center of mass of the triatomic system. Three Jacobi angles complete the description of the system: θ (the angle between r and ρ), γ (the angle between ρ and R), and β (the polar angle between the triatom plane and R). The calculations reported here are characterized by the use of the additional 5D *polar angle*-averaged potential energy surface

$$\bar{U}(r\rho R\theta\gamma) = \frac{1}{\pi}\int_0^\pi U(r\rho R\theta\gamma\beta)d\beta \tag{10}$$

instead of the original full 6D potential $U(r\rho R\theta\gamma\beta)$.

In order to calculate ψ_λ (and χ_{λ_0}) within a 4D infinite-order-sudden-approximation (IOSA) approach, the following Hamiltonian should be considered:[21]

$$H = -\frac{\hbar^2}{2mr}\frac{\partial^2}{\partial r^2}r - \frac{\hbar^2}{2\mu\rho}\frac{\partial^2}{\partial\rho^2}\rho - \frac{\hbar^2}{2\mathrm{MR}}\frac{\partial^2}{\partial R^2}R + \left(\frac{1}{2\mu\rho^2} + \frac{1}{2mr^2}\right)\vec{J}^2 + \left(\frac{1}{2\mu\rho^2} + \frac{1}{2MR^2}\right)\vec{\mathrm{K}}^2 + \frac{\hbar^2 J(J+1)}{2MR^2} + U(r\rho R\theta\gamma|\beta) \tag{11}$$

where the averaged potential energy surface $\bar{U}$ may also be used instead of U, and m, μ, and M are, respectively, the reduced masses of the diatomic bond, triatomic molecule, and whole atom + triatom system. On the other hand, $\vec{j}$ and $\vec{K}$ represent, respectively, the bending and rotational angular momentum operators of the triatomic molecule, respectively; as before, J denotes the total angular momentum quantum number. It should also be mentioned that eq 11 is the result of applying the close-coupled states (or j_z)[14,22] approximation to a more general expression of H.[15,21]

In general we distinguish between the asymptotic region and the short interaction region. The SE that follows by employing the Hamiltonian defined in eq 11 is then treated twice: once to calculate the asymptotic (unperturbed) elastic wave function ψ_λ, and once to calculate χ_{λ_0}. In this paragraph we start by considering the expression of the (unperturbed) potential energy surface to be used for the solution of ψ_λ (see eq 6). It is given by

$$U(r\rho R\theta|\beta) = v(r\rho\theta) + w(R|\beta) \tag{12}$$

where $v(r\rho\theta)$ is the potential energy surface of the O_3 molecule which follows from

$$v(r\rho\theta) = \lim_{R\to\infty} U(r\rho R\theta\gamma\beta) \tag{13}$$

and the distortion potential $w(R|\beta)$ may be defined as an eigenvalue of the following rotational SE

$$\left[\left(\frac{1}{2\mu\rho_e^2} + \frac{1}{2MR^2}\right)\vec{K}^2 + U(r_e\rho_e R\theta_e\gamma|\beta) - w(R|\beta)\right]h(\gamma|\beta) = 0 \tag{14}$$

Note that ρ_e, r_e, and θ_e are obtained from the equilibrium properties[23] of the O_3 molecule, which is an integral part of the HO_3 potential energy surface,[17] while β is an IOSA angle.[15,24,25]

In a 3D reduced dimensionality treatment where the angular directions are fixed, $\vec{K} \equiv 0$, and hence it results from eq 14 that

$$w(R|\beta) = U(r_e\rho_e R\theta_e\gamma|\beta) \tag{15}$$

In order to eliminate the functional dependence of w in β and γ from eq 15, we may take β as a fixed (IOSA) parameter or rather turn it out by means of the average potential $\bar{U}$ in eq 5. Recall that in the IOSA model γ may be taken as a fixed parameter or one may choose to average U in eq 15 in terms of cos γ over the range $(0, \pi)$, as it has been done elsewhere.[6,21] Note that this last averaging of U is equivalent to weighting the potential with the lowest order of the spherical harmonics $y_{0,0}(\gamma|\beta)$, while it would be rather more realistic to do the weighting by using $h(\gamma|\beta)$ defined in eq 14. Since $h(\gamma|\beta)$, an eigenfunction of eq 14, is an undulating function which has

maxima where U has minima, it looks therefore more appropriate (without having to resort to the formal solution of eq 14) that one approximates the averaging of U over $h(\gamma|\beta)$ by adopting the minimum value of this potential in the range of $0 \leq \gamma \leq \pi$. We are then led in this analytical way to introduce (as in ref 13) the angle γ_{MP} which is defined as the minimum of $U(Rr_e\rho_e\theta_e\gamma|\beta)$ with respect to γ. In practice, it is determined by imposing the condition of extremum given by

$$\frac{\partial}{\partial\gamma} U(Rr_e\rho_e\theta_e\gamma|\beta)|_{\gamma=\gamma_{MP}} = 0 \qquad (16)$$

Similarly, γ_{SP} is obtained if $\bar{U}$ is used instead of U in eq 16.

The function χ_{λ_0} is derived by solving eq 8 in the reagents AC. For this purpose the range of the reagents vibrational coordinate(s) are enlarged such as to comprise the relevant reactive regions and include the necessary decoupling NIPs. In the title reactive system, there is one preferred open channel,[16,18] and hence one of the extreme bonds O_2 in the O_3 molecule remains essentially unbroken through the whole reactive process. To account for this possibility, two negative imaginary terms are added to the real Hamiltonian: a vibrational term along the distance ρ and another translational term along R, namely

$$V_I(r, \rho, R) = -i[v_{I\rho}(\rho) + v_{IR}(R)] \qquad (17)$$

The addition of the NIPs to the real averaged potential $\bar{U}$ converts the scattering problem into a bound system problem, and hence makes χ_{λ_0} expandable in terms of square integrable L^2 functions.[26,27] These functions are chosen here as localized functions for the translational components and adiabatic basis sets for the vibrational ones. Thus,

$$\chi^J_{\lambda_0}(r\rho R\theta\gamma|j) = \frac{1}{r\rho R}\sum_{n\lambda} a^J_{n\lambda} g(R|n) f(r\rho\theta\gamma|j|n\lambda) \qquad (18)$$

where $g(R|n)$ represents the translational component which is chosen to be a standard Gaussian function of the form

$$g(R|n) = \left(\frac{\alpha}{\sigma\sqrt{\pi}}\right)^{1/2} \exp\left[-\frac{\alpha^2}{2}\left(\frac{R-R_n}{\sigma}\right)^2\right] \qquad (19)$$

where σ is the translational step size

$$\sigma = R_n - R_{n-1} \qquad (20)$$

Regarding $f(r\rho\theta\gamma|j|n\lambda)$, this is an eigenfunction of the *3*D Schrödinger equation

$$\left[-\frac{\hbar^2}{2mr}\frac{\partial^2}{\partial r^2} r - \frac{\hbar^2}{2\mu\rho}\frac{\partial^2}{\partial\rho^2}\rho + \left(\frac{1}{2mr^2} + \frac{1}{2\mu\rho^2}\right)\vec{J}^2 + U(r\rho R_n\theta\gamma|\beta) - \epsilon(\lambda|\theta\gamma j|R_n)\right] f(r\rho\theta\gamma|j|n\lambda) = 0 \qquad (21)$$

Once eq 21 has been solved, it is then possible, starting from eq 5, to obtain the nonreactive S-matrix element. Finally, from the J-specific averaged reaction probabilities, the QM total reactive cross sections are calculated by using

$$\sigma^r(E_{tr}, \lambda_0) = \frac{\pi}{k^2(E_{tr})}\sum_J (2J+1) P^J_{react}(E_{tr}, \lambda_0) \qquad (22)$$

TABLE 1: Calculated Reactive Cross Sections with $N = 2$ (in a_0^2) for the Reaction H + O_3 → HO + O_2

	front path		rear path		average	
energy (eV)	SP	MP	SP	MP	SP	MP
0.035		2.14		2.85		2.50
0.050	0.05	3.03		3.41	0.04	3.22
0.075	0.22	4.05	0.05	3.97	0.19	4.01
0.100	1.01	6.85	1.01	7.80	1.01	7.33
0.150	1.14	7.16	1.03	8.12	1.12	7.64
0.200	3.81	9.64	1.06	12.05	3.38	10.85
0.250	8.01		2.30		7.12	
0.300	14.10		2.61		12.31	

where $k(E_{tr})$ is the standard wave number for the whole atom + triatom system, which is defined by $k^2(E_{tr}) = 2M/\hbar^2\, E_{tr}$, and the reactive probability P^J_{react} is calculated for each integer value of J by means of eq 3.

3. Numerical Details

In this work, we have carried out quantum dynamical computations of nonreactive probabilities for the H + O_3 collisional process over the range of translational energies $0.035 \leq E_{tr}/\text{eV} \leq 0.300$ using the DMBE HO_3 potential energy surface of Varandas and Yu.[17] The reactive probabilities have then been computed by means of eq 3, and the total reactive cross sections by using eq 22. The calculations have generally been carried out within the j_z-approximation using either a polar-averaged expression of the potential energy surface (see eq 10) or rather a multiple-path expression of the same function, using the polar angle β as the external parameter. However, in order to derive the total wave function in the reagents' AC Ψ_{λ_0} (eq 5), the parameter γ has been treated as a pseudo-IOSA parameter, when at each translational distance R its value is replaced by one of the solutions of eq 16 for each one of the M(S)P approaches used here.

To solve eq 8 in an adequate way (for a given ψ_{λ_0}), the R-translational axis has been required to be divided into up to 110 equidistant sectors. In each of these one Gaussian, standing as a translational basis function, and a set of twofold adiabatic vibrational basis functions have been used (see eq 18). The number of such functions varies from one sector to another, but at each sector their number is constrained by a simple energy cutoff of 0.5 eV.[21,27] This implied at the end, to solve about 5000 complex equations in order to obtain the mentioned coefficients.

We note that a particularly difficult task has been to solve eq 16 for a single $\gamma_{M(S)P}$ when, as we know, the title reaction is characterized by having more than one reaction track: two due to the two attacking angles, and another two because of the competitive reaction (eq 1). It is quite obvious that, once chosen a determined track, it is forbidden to mix them in between different R-translational steps. This selection has been done in the present work by applying a particular mask delimiting, for each case, the range of allowed values for γ.

4. Results

Calculations obtained for the reactive cross sections in the title reaction using the approaches mentioned in this paper are shown in Tables 1−4, and Figure 1. Previously published QCT and IOSA results are also given in Table 4 for comparison. In Figure 1 and Table 4, N denotes the number of polar angles

TABLE 2: Calculated Reactive Cross Sections with $N = 3$ (in a_0^2) for the Reaction $H + O_3 \rightarrow HO + O_2$

	front path		rear path		average	
energy (eV)	SP	MP	SP	MP	SP	MP
0.035						
0.050	0.14	3.23		2.32	0.12	2.78
0.075	0.19	4.98	0.07	3.00	0.17	3.19
0.100	0.88	6.87	1.02	5.50	0.90	6.19
0.150	3.26	7.60	0.97	8.03	2.92	7.82
0.200	7.45	10.69	1.20	11.64	6.45	11.17
0.250	8.90		1.70		7.75	
0.300			3.90			

TABLE 3: Calculated SP Reactive Cross Sections with $N = 10$ (in a_0^2) for the Reaction $H + O_3 \rightarrow HO + O_2$

energy (eV)	front path	rear path	average
0.050	1.75		1.04
0.075	2.01	0.08	1.23
0.100	3.12	0.83	2.19
0.150	4.85	2.03	3.71
0.200	7.34	4.99	6.39

TABLE 4: Calculated Reactive Cross Sections in a_0^2 for the Reaction $H + O_3 \rightarrow HO + O_2$[a]

		$N = 2$		$N = 3$		$N = 10$	
energy (eV)	QCT[18]	SP	MP	SP	MP	SP	IOSA[16]
0.015	1.68						
0.025	2.28						
0.030	3.06						
0.035	3.38		2.50				
0.050	3.80	0.04	3.22	0.12	2.78	1.04	0.10
0.075	4.87	0.19	4.01	0.17	3.99	1.23	
0.100	6.67	1.01	7.33	0.90	6.19	2.19	0.50
0.150		1.12	7.64	2.92	7.82	3.71	3.16
0.200	10.39	3.38	10.85	6.45	11.17	6.39	5.42
0.250		7.12		7.75			9.12
0.300	14.25	12.31					12.62
0.350							15.94
0.400							18.87
0.500	19.00						
0.700	26.61						

[a] Only the average values are reported both for the SP and MP methods.

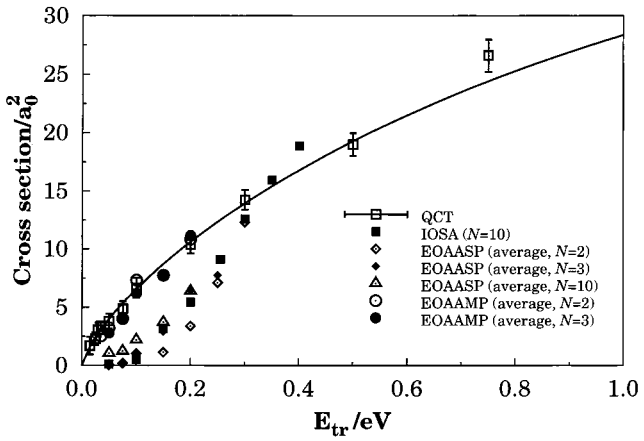

Figure 1. A comparison of the cross section as a function of the translational energy for the process $H + O_3 \rightarrow OH + O_2$ for the different theories mentioned in this paper. The new results have been computed for values of E_{tr} ranging from 0.035 to 0.30 eV.

over which the computed potential U (SP) or cross sections (MP) have been averaged. Note also that in Tables 1−3, the labeling of results as belonging to the "front" and "rear" tracks means that they were located in the ranges $0 \leq \gamma < \pi/2$ and $\pi/2 \leq \gamma \leq \pi$, respectively. In order to find the average of cross sections calculated in different tracks (front and rear), we have made use of the quantum mechanical interpretation of the wave amplitude $h(\gamma|\beta)$ defined in eq 14. In fact, we expect it to have maximum values where U has a minimum. The probability that the molecule is at certain $\gamma_{M(S)P}$ (and hence in the respective track) is then proportional to the value of the cross section at the highest studied translational energy,

$$p(\gamma_{M(S)P}) \sim |h(\gamma|\beta)|^2 \tag{23}$$

The closest value to $p(\gamma_{M(S)P})$ in eq 23 of the present calculations, without solving explicitly eq 14, is given by

$$p(\gamma_{M(S)P}) \sim \sigma^r(E_{tr} \rightarrow \infty, \lambda_0) \tag{24}$$

where we have taken E_{tr} in eq 23 as tending to ∞, since we then expect σ^r to become independent of energy fluctuations. The notable feature from Table 4 and Figure 1 is the fact that the average SP and MP quantum results seem to be pretty well converged for $N = 3$, and hence are likely to represent realistic estimates of the true values. Also interesting is the good agreement between the MP results and the QCT calculations over the range of translational energies where they overlap.

Once obtained the energy dependence of the reactive cross sections, one is able to deduce the corresponding rate constant by means of the well-known formula

$$k(T) = f\left(\frac{8k_BT}{\pi M}\right)^{1/2}\left(\frac{1}{k_BT}\right)^2 \int_0^\infty E_{tr}\sigma^r \exp(-E_{tr}/k_BT)\, dE_{tr} \tag{25}$$

where M is the reduced mass of the atom−triatom colliding pair, k_B is the Boltzmann constant, and f is the appropriate electronic degeneracy factor which for the title reaction is equal to one.

In order to solve eq 25, we follow a previous procedure[16] which consists of fitting the calculated cross sections to the form

$$\sigma^r = \frac{C}{E^n}\exp(mE) \tag{26}$$

where C, m, and n are least-squares parameters. Equation 26 is then introduced in eq 25 leading to the exact form[18,28]

$$k(T) = C\left(\frac{8k_BT}{\pi\mu}\right)^{1/2}\frac{(k_BT)^n\Gamma(n+2)}{(1+mk_BT)^{n+2}} \tag{27}$$

Avoiding the description of numerical details, the results are displayed graphically in Figure 2. One may observe by comparing their relative behavior that the calculated $k(T)$ follow the same trend as in the case of the cross sections results reported above.

5. Conclusions

We have carried out 3D quantum dynamics calculations of the reaction $H + O_3 \rightarrow HO + O_2$ using a recently reported[17] DMBE potential energy surface for the ground electronic state of HO_3. Two different adiabatic concepts have been applied in developing the QM models. One, the SP approach, led to lower values of cross sections than those predicted by the QCT theory, especially near threshold, but still better than those obtained

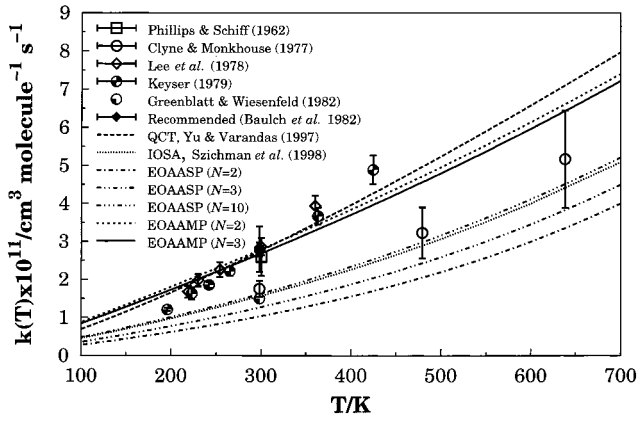

Figure 2. Rate constants for the reaction H + O_3 → OH + O_2. Experimental results are from refs 29−34, while the QCT and IOSA values are from refs 8 and 16, respectively.

from the IOSA model. The other, the MP approach, yielded results in quite good agreement with previous QCT results. The difference between SP and MP approaches is in some extent comparable to the way the average of the square modulus of the sum of two wave functions is done, i.e.,

$$|<\Psi_1 + \Psi_2>\mathrm{av}|^2 \tag{28}$$

or

$$<|\Psi_1|^2 + |\Psi_2|^2>\mathrm{av} \tag{29}$$

Equation 28 and 29 will be identical if

$$\Psi_1 \approx \Psi_2 \tag{30}$$

although eq 29 becomes as high as twice that from eq 28 if one of the Ψs is predominant over the other. Equation 30 expresses the condition of homogeneity of the PES, but also for high values of E_{tr} will the same expression apply, as a consequence of high translational energies tending to smear down the influence of the topographical details of the potential energy surface.

In conclusion, the adiabatic approaches M(S)P may be used as complementary to the known IOSA methods, specially in the study of QM characteristics of chemical reactions at low translational energies. Particularly, the SP is more advantageous over the similar MP approach, considering the computation time required by both procedures. Nevertheless, it is difficult to state at the present stage, what of both methods is best justified quantum mechanically. More computational experiments are thus requested in order to get a final judgment.

Acknowledgment. This work has been supported by the Fundação para a Ciência e Tecnologia, Portugal, under programmes PRAXIS XXI and FEDER.

References and Notes

(1) (a) Zhang, J. Z. H.; Miller, W. H. *Chem. Phys. Lett.* **1988**, *153*, 465. (b) Zhang, J. Z. H.; Miller, W. H. *Chem. Phys. Lett.* **1989**, *159*, 130. (c) Zhang, J. Z. H.; Miller, W. H. *J. Chem. Phys.* **1989**, *91*, 1528.
(2) Mielke, S. L.; Lynch, G. C.; Truhlar, D. G.; Schwenke, D. W. *J. Phys. Chem.* **1994**, *98*, 8000.
(3) Neuhauser, D.; Judson, R. S.; Jaffe, R. L.; Baer, M.; Kouri, D. J. *Chem. Phys. Lett.* **1991**, *176*, 546.
(4) Haug, K.; Schwenke, D. W.; Truhlar, D. G.; Zhang, Y.; Zhang, J. Z. H.; Kouri, D. J. *J. Chem. Phys.* **1987**, *87*, 1892.
(5) Takana, Sh.; Tsuda, K-i.; Ohsaki, A.; Nakamura, H. *Advances in Molecular Vibrations and Collision Dynamics*; Bowman, J. M., Ed.; JAI Press: Greenwich, CT, 1994; Vol. 2A, p 245.
(6) Baer, M.; Last, I.; Loesch, H.-J. *J. Chem. Phys.* **1994**, *101*, 9648.
(7) Manthe, U.; Seideman, T.; Miller, W. H. *J. Chem. Phys.* **1994**, *101*, 4759.
(8) Neuhauser, D. *J. Chem. Phys.* **1994**, *100*, 9272.
(9) Zhang, D. H.; Zhang, J. Z. H. *J. Chem. Phys.* **1994**, *100*, 2697.
(10) Zhang, D. H.; Light, J. C. *J. Chem. Phys.* **1996**, *104*, 4544.
(11) (a) Zhu, W.; Zhang, J. Z. H.; Zhang, Y. C.; Zhang, Y. B.; Zhang, L. X.; Zhang, D. H. *J. Chem. Phys.* **1998**, *108*, 3509. (b) Zhu, W.; Zhang, J. Z. H.; Zhang, D. H. *Chem. Phys. Lett.* **1998**, *292*, 46.
(12) Szichman, H.; Baer, M.; Nakamura, H. *J. Chem. Phys.* **1997**, *107*, 3521.
(13) Varandas, A. J. C.; Szichman, H. *Chem. Phys. Lett.* **1998**, *295*, 113.
(14) Pack, R. T. *J. Chem. Phys.* **1974**, *60*, 633.
(15) Szichman, H.; Baer, M.; Varandas, A. J. C. *J. Phys. Chem.* **1997**, *101*, 8817.
(16) Szichman, H.; Baer, M.; Varandas, A. J. C. *J. Phys. Chem.* **1998**, *102*, 8909.
(17) Varandas, A. J. C.; Yu, H. G. *Mol. Phys.* **1997**, *91*, 301.
(18) Yu, H. G.; Varandas, A. J. C. *J. Chem. Soc., Faraday Trans.* **1997**, *93*, 2651.
(19) Zhang, J. Z. H.; Kouri, D. J.; Haug, K.; Schwenke, D. W.; Shima, Y.; Truhlar, D. G. *J. Chem. Phys.* **1988**, *88*, 2492.
(20) Neuhauser, D.; Baer, M. *J. Chem. Phys.* **1989**, *90*, 4351.
(21) Szichman, H.; Baer, M. *J. Chem. Phys.* **1994**, *101*, 2081.
(22) McGuire, P.; Kouri, D. J. *J. Chem. Phys.* **1974**, *60*, 2488.
(23) Murrell, J. N.; Sorbie, K. S.; Varandas, A. J. C. *Mol. Phys.* **1976**, *32*, 1359.
(24) Szichman, H.; Varandas, A. J. C.; Baer, M. *Chem. Phys. Lett.* **1994**, *231*, 253.
(25) Szichman, H.; Baer, M. *Chem. Phys. Lett.* **1995**, *242*, 285.
(26) Szichman, H.; Last, I.; Baram, A.; Baer, M. *J. Phys. Chem.* **1993**, *97*, 6436.
(27) Last, I.; Baram, A.; Szichman, H.; Baer, M. *J. Phys. Chem.* **1993**, *97*, 7040.
(28) LeRoy, R. L. *J. Chem. Phys.* **1969**, *73*, 4338.
(29) Phillips, L. F.; Schiff, H. I. *J. Chem. Phys.* **1962**, *37*, 1233.
(30) Baulch, D. L.; Cox, R. A.; Crutzen, P. J.; Hampson R. F., Jr.; Kerr, J. A.; Troe, J.; Watson, R. T. *J. Phys. Chem. Ref. Data* **1982**, *11*, 327.
(31) Clyne, M. A. A.; Monkhouse, P. B. *J. Chem. Soc., Faraday Trans. 2* **1977**, *73*, 298.
(32) Lee, J. H.; Michael, J. V.; Payne, W. A.; Stief, L. J. *J. Chem. Phys.* **1978**, *69*, 350.
(33) Keyser, L. F. *J. Phys. Chem.* **1979**, *83*, 645.
(34) Greenblatt, G. D.; Wiesenfeld, J. R. *J. Geophys. Res.* **1982**, *87*, 11145.